CrossMark

ORIGINAL PAPER

Glenoid morphology and the safe zone for protecting the suprascapular nerve during baseplate fixation in reverse shoulder arthroplasty

Yuhui Yang[1] · Jianlin Zuo[1] · Tong Liu[1] · Pu Shao[1] · Haihe Wu[1] · Zhongli Gao[1] (ID) · Jianlin Xiao[1]

Abstract

Purpose The purpose of this study was to investigate glenoid morphology and define the safe zone for protecting the suprascapular nerve baseplate screw during baseplate fixation in reverse shoulder arthroplasty (RSA) in a Chinese population.

Methods Shoulder computed tomography (CT) scans from 56 subjects were retrospectively reviewed. Three-dimensional (3D) reconstruction was performed using Mimics software, and corresponding bony references were used to evaluate glenoid morphology. To standardize evaluation, the coronal scapular plane was defined. Safe fixation distances and screw placements were investigated by constructing a simulated cutting plane of the baseplate during RSA.

Results Mean glenoid height was 35.83 ± 2.95 mm, and width was 27.32 ± 2.78 mm, with significant sexual dimorphism ($p < 0.01$). According to the cutting plane morphology, the average baseplate radius was 13.84 ± 1.34 mm. The distances from the suprascapular notch and from two bony reference points at the base of the scapular spine to the cutting plane were 30.27 ± 2.77 mm, 18.39 ± 1.67 mm and 16.52 ± 1.52 mm, respectively, with a gender-related difference. Based on the clock face indication system, the danger zone caused by the suprascapular nerve projection was oriented between the two o'clock and eight o'clock positions in reference to the right shoulder.

Conclusions Glenoid size and the safe zone for screw fixation during RSA were characterized in a Chinese population. Careful consideration of baseplate fixation and avoidance of suprascapular nerve injury are important for improved clinical outcome.

Introduction

Reverse shoulder arthroplasty (RSA) has been widely used as a cost-effective surgical treatment with positive clinical outcomes to relieve pain and restore function in patients with severe rotator cuff arthropathy and glenohumeral arthritis [1–3]. Importantly, optimal implant positioning and ability to restore the original anatomy contributes to improved implant quality and fewer complications.

When implanting the glenoid component, considerations should be made for the suprascapular nerve due to its unique anatomy and the difficulty of its identification in rotator cuff arthropathy. This nerve arises from the C5 and C6 nerve roots, traveling towards the superior glenoid rim at the level of the suprascapular notch. After entering the supraspinous fossa, it curves around the base of the scapular spine at the spinoglenoid notch, then runs away from the inferior glenoid rim in a medial direction (Fig. 1). Given the route of the suprascapular nerve along the posterior surface of the scapula, surgeons should pay close attention to avoid nerve injury during placement of the fixation screws in the neck of the scapula [4, 5].
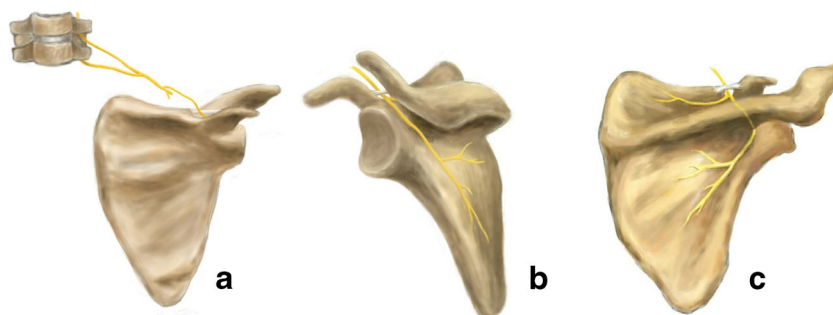
Neurological complications of RSA have been reported with an incidence of 0.6–3.6% [6, 7], which is higher than

✉ Zhongli Gao
zhongligao@sina.com

✉ Jianlin Xiao
xiaojianlin10@qq.com

1 Department of Orthopaedics, China–Japan Union Hospital of Jilin University, Changchun, Jilin, China

anatomic total shoulder arthroplasty, possibly due to the requirement of securing the glenoid component with multiple screws [6]. A cadaveric study by Molony et al. [8] demonstrated that prominent posterior and superior screws could damage or over-penetrate the suprascapular nerve when drilling. Similarly, Wang et al. [9] reported a case of suprascapular neuropathy secondary to RSA, caused by a perforating superior screw. Hart et al. [10] concluded, also with a cadaveric study, that either the suprascapular nerve or artery was vulnerable to injury by the posterior fixation screw. Injury to the nerve could lead to increased post-operative pain and suboptimal outcomes, which could demand further medical intervention [11]. A better understanding of glenoid morphology and adjacent anatomic structures is necessary to ensure proper sizing and correct placement of prosthetic components, which would contribute to minimizing complications and reducing the rates of implant failure [6, 12].

Previous anatomic evaluations, shedding light on facilitating RSA and avoiding implant complications have been conducted using human cadavers or isolated scapular bones [8, 10, 13–15]. However, the morphological measurements in most cadaveric studies were based on the glenoid surface, instead of the cutting plane of RSA. In addition, there have been few studies recommending the drilling distances and location of the safe zone for screw placement during RSA, especially in the Chinese population. Three-dimensional (3D) reconstruction and simulated surgical segmentation have been confirmed to be effective and accurate in both preoperative planning [16, 17] as well as prosthesis design [18]. Therefore, the present study was conducted using 3D reconstruction techniques to evaluate the geometry of the glenoid surface in a healthy Chinese population, and to define the safe zone as well as the appropriate length of fixation screws to avoid injury of the suprascapular nerve during RSA.

Materials and methods

Study subjects

The study was approved by the institutional review board of China–Japan Union Hospital of Jilin University. Shoulder

computed tomography (CT) scans from patients who attended our hospital for the diagnosis of proximal humeral fractures from January 2013 to December 2016 were retrospectively reviewed from the hospital Picture Archiving and Communication System (PACS) database. A total of 56 normal shoulders (average patient age: 53.09 years, range: 35–75 years) were included for analysis, whereas 37 shoulders were excluded due to glenoid fractures, surgical history, or degenerative changes.

Image analysis and measurements

Shoulder CT scans were performed with a Toshiba brand Aquilion CT scanner (120 kVp; 320 mA; 512 × 512 matrix; slice thickness, 1.0 mm) at the China–Japan Union Hospital of Jilin University. All slices were saved in Digital Imaging and Communications in Medicine (DICOM) format, and imported into Mimics 17.0 software (Materialize, Leuven, Belgium) for 3D reconstruction. As previously reported [19], four extreme glenoid poles of the glenoid articular surface were selected on each scapular model. The height (h) and width (w) of the glenoid fossa were measured to determine the glenoid size (Fig. 2a). Following simulated segmentation, the glenoid surface was marked and the surface centre (O) was calculated as its centre of gravity [19, 20]. The coronal scapular plane [19] was defined to standardize the position of the shoulder model, which involved the inferior angle of the scapula (IA), the scapula trigonum (ST) (junction of the scapular spine and medial scapular border), and the center of the glenoid surface (Fig. 2b). The transverse axis was defined as a line connecting the scapula trigonum and the center of the glenoid. According to previous literature [12, 20], it is recommended that the RSA component be placed at 10° of inferior inclination to reduce scapular notching and mechanical failure. Herein, a corresponding cutting plane was generated with respect to the transverse axis in both 2D and 3D imaging environments (Fig. 2c and d).

Given the anatomic trajectory of the suprascapular nerve, one bony reference point at the level of the suprascapular notch (A) and two bony reference points at the base of the scapular spine (B, C) were selected (Fig. 3). The 3D model and simulated cutting plane were then imported into 3-Matic

Fig. 2 **a** The anatomical landmarks on each scapular model are the glenoid poles, used to measure the glenoid fossa height (h) and width (w). The *green* meshed model is the glenoid surface, and *point* O is the calculated glenoid surface centre. **b** The coronal scapular plane: three points (connected by *black dotted lines*) placed at the inferior angle (IA) of the scapula, the scapula trigonum (ST), and the centre of the glenoid surface (O). **c** In a 2D coronal scapular plane, the simulated cutting plane was constructed at 10° of inferior inclination according to the transverse axis. **d** The 3D reconstructed image of the simulated cutting plane and scapular model
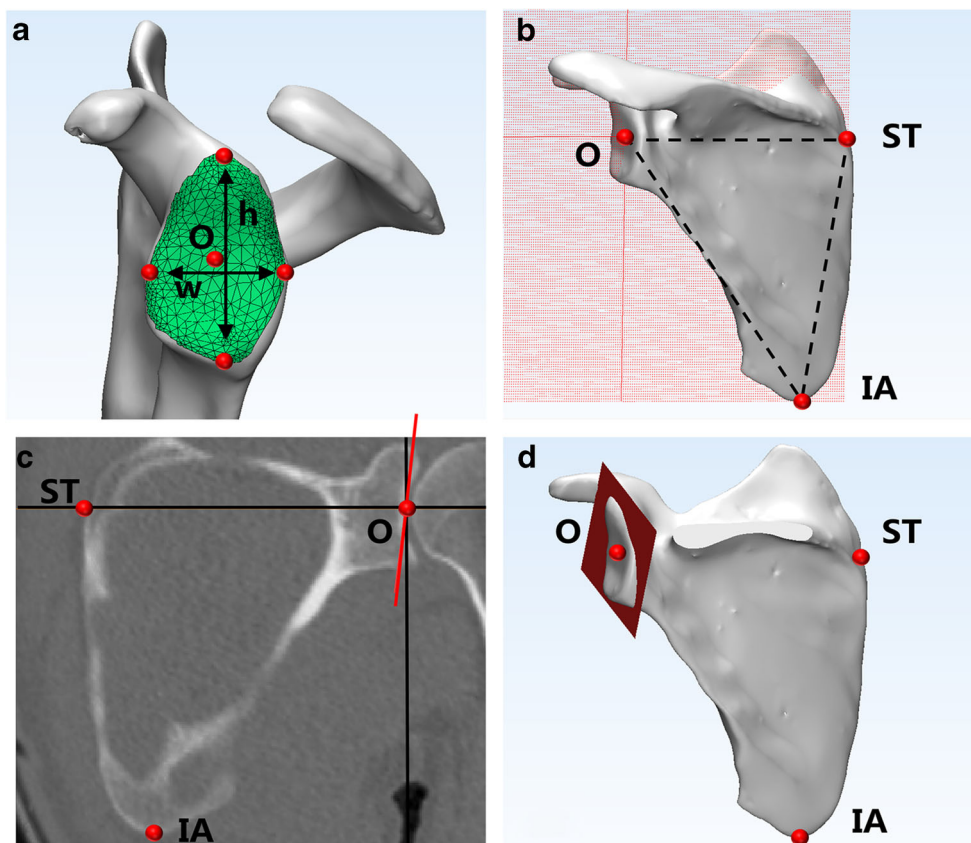
9.0 software (Materialize, Leuven, Belgium). Accordingly, the best-fit circle of the cutting plane was determined, and measured as a morphological index of the glenoid fossa. In the present study, the best-fit circle (glenoid baseplate) was
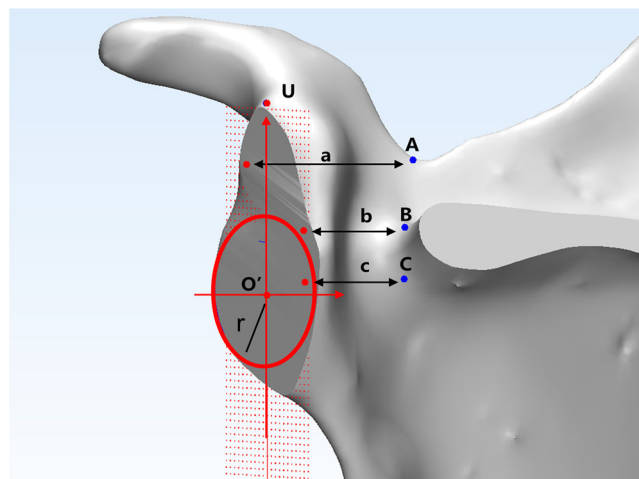

Fig. 3 Simulated cutting plane and projections of corresponding bony reference points. The *red plane* represents the cutting plane, and the corresponding bone was removed. The *red circle* represents the best-fit circle. *Point A* is the suprascapular notch. *Points B and C* are the bony border at the base of the scapular spine, at the spinoglenoid notch. *Point U* is the superior point of glenoid rim, and *point O′* is the centre of the best-fit circle with the radius of r. *a*, *b* and *c* represent the corresponding safe distances

placed as inferiorly as possible to prevent notching [21]. Based on the superior point of the glenoid rim (U) and the centre of baseplate circle (O′) as suggested [14, 22], a line was drawn to act as the Y axis and to establish the projected coordinate system. Subsequently, the bony reference points were projected to the cutting plane to characterize the safe zone and limiting distance for inserted screws.

Statistical analysis

All data were categorized according to gender and side of the body (left or right), and differences were assessed using independent sample t-tests. Correlations between two continuous indices were analyzed using Spearman's correlation coefficient. For assessing inter-observer reliability, two analysts performed point selection and corresponding measurements independently. For assessing intra-observer reliability, measurements were repeated one month later by the same analysts. Intraclass correlation coefficient was used to calculate inter-observer and intra-observer effects. A post-hoc power calculation was determined by the statistical power analyses G Power 3.1 [23] to eliminate type II error. All statistical analyses were performed using SPSS version 21.0 (SPSS, Chicago, IL, USA), and a *p* value <0.05 was considered statistically significant.

Results

The anatomy of the glenohumeral joint and corresponding bony structures were evaluated following 3D reconstruction. The size of the glenoid fossa and the projection distance from the bony reference points towards the cutting plane are summarized in Table 1. Intraclass correlation coefficient results of the intra-observer and inter-observer reliabilities for all the measurement indices, evaluated by the one-way random effects model, ranged from 0.94 to 0.97 and from 0.87 to 0.95, respectively. Post-hoc power analysis showed a power > 0.78 for detecting a significant difference.

With respect to the safe screw distance, the limit for the distance from the cutting plane to the nerve at the suprascapular notch was 25.43 mm, and to the base of the scapular spine was 13.38 mm. No significant difference was observed between the left and right shoulders. However, all indices measured in the present study confirmed significant gender differences (Table 2). As listed, the measurements in men were significantly larger than those in women ($p < 0.05$), in both glenoid size and safe distances. Further, the safe zone of the scapulae of men was within 26.57 mm for distance a, and 13.83 mm for distance c, while the corresponding distances of women were within 25.43 mm and 13.38 mm, respectively. There was high correlation between the glenoid height and width ($r = 0.77$, $p = 0.00$). The correlation indices calculated between the height or width, compared to the radius were 0.813 and 0.992, respectively. In addition, the correlation indices regarding safe distances are summarized in Table 3.

The projections of the bony reference points were presented as dot plot (Fig. 4). Based on the coordinate system described above, the danger zone caused by the suprascapular nerve projection was oriented between the two o'clock and eight o'clock positions in reference to the right shoulder. With the origin of coordinates, a standard baseplate is also depicted. Accordingly, the projection areas of B and C (Fig. 4) were

Table 1 The projection distance measurements from bony reference points towards the cutting plane

Parameters	Mean ± SD (mm)	95% CI (mm)	Range (mm)
h	35.83 ± 2.95	35.04–36.62	30.98–43.26
w	27.32 ± 2.78	26.57–28.06	22.62–34.42
r	13.84 ± 1.34	13.48–14.20	11.54–17.21
a	30.27 ± 2.77	29.53–31.02	25.43–37.61
b	18.39 ± 1.67	17.94–18.83	15.02–22.59
c	16.52 ± 1.52	16.11–16.92	13.38–19.72

SD standard deviation, *CI* confidence interval

Parameter definitions: h, height of the glenoid fossa; w, width of the glenoid fossa; r, radius of the best-fit circle (baseplate); a, b, and c, safe distances of projections to the cutting plane from A, B and C, respectively; A, suprascapular notch; B and C, bony border of the base of the scapular spine

defined as danger zone I, which was mainly at risk of the posterior screw, while the projection area of A was defined as danger zone II and was associated with risk from the superior screw.

Discussion

Glenoid morphological evaluation and the optimization of baseplate fixation are important for a successful RSA procedure. In the present study, we measured the glenoid fossa and proposed the definition of a safe zone for avoiding injury to the suprascapular nerve caused by penetrating screws during RSA in a Chinese population.

Compared with conventional two-dimensional radiographs, 3D reconstructions from CT scans are independent of scapular orientation, allowing for more accurate measurement and pre-operative planning [24, 25]. In addition, several biomechanical studies concerning screw configuration and component position have demonstrated that inferior tilt of the baseplate is associated with reduced scapular notching [12, 26] and provides better biomechanical fixation [20]. Therefore, accurate screw drilling distances and safe zone identification cannot be obtained through simple cadaveric studies, which are measured in reference to the glenoid surface. Compared to the limited sample source of cadaveric subjects, CT-based models are more accessible and accurate for safe zone definition and personalized pre-operative planning. To our knowledge, this is the first study to present quantitative 3D morphological analysis and safe zone measurements concerning screw fixation in RSA, especially for a Chinese population.

Surgeons have been concerned that the size of commercially available RSA baseplates were too large for the Asian population [21, 27], but few anatomical studies have addressed these concerns. Our data showed that the average glenoid height and width were 35.8 mm and 27.3 mm, and highly correlated with each other ($r = 0.769$). In comparison, the glenoid dimensions in other populations have been reported as 39.5 mm and 31.0 mm in the United States [28], 41.3 mm and 29.4 mm in France [29], 31.5 mm and 23.1 mm in Japan [30], and 36.6 mm and 27.8 mm in Switzerland [31]. In addition, we demonstrated that glenoid size was significantly larger in men compared to women, which confirmed the previous finding that gender is the strongest independent predictor of glenoid size [32]. In our study, the average diameter of the best-fit circle was 27.7 mm, which is smaller than the standard 29-mm baseplate. An anatomical and clinical study in a Korean population [21] arrived at similar conclusions, and indicated difficulty in inserting the standard baseplate intra-operatively, especially in some female patients. Implantation of an oversized baseplate can result in insufficient bone-implant contact and bone stock for screw fixation. Furthermore,

Table 2 Gender differences in glenoid morphology measurements

Parameter	Height (mm)		Width (mm)		Radius (mm)		a (mm)		b (mm)		c (mm)	
	M	F	M	F	M	F	M	F	M	F	M	F
Mean	38.14	34.22	29.65	25.69	14.96	13.06	31.84	29.18	19.13	17.87	17.07	16.13
Variance	2.30	2.20	2.38	1.66	1.14	0.81	2.83	2.18	1.64	1.51	1.27	1.57
Minimum	33.50	30.98	25.07	22.62	12.81	11.54	26.57	25.43	15.51	15.02	13.83	13.38
Maximum	43.26	39.61	34.42	29.70	17.21	14.93	37.61	34.90	22.59	21.05	19.72	19.27
p value	0.00		0.00		0.00		0.00		0.01		0.02	

Abbreviations: M, male; F, female; a, b, and c, safe distances of projections to the cutting plate from A, B and C, respectively; A, suprascapular notch; B and C, bony border of the base of the scapular spine

oversized baseplates have been reported to cause more micromotion and less impingement-free range of motion [33], which would likely lead to early glenoid loosening. Accordingly, the quantitative analysis in the present study will be useful to determine the size of RSA implants and to improve the clinical outcomes of shoulder arthroplasty for Chinese patients.

Rigid and safe screw fixation in RSA is achieved by pursuing deeper bone stock while avoiding injuries to the adjacent neurovascular structures. Normal glenoid version inclination varies over a wide range of values [34], thus the glenoid surface may not be an appropriate choice for the analysis of safe screw fixation in RSA. As summarized in Table 4, several previous studies on human cadavers have addressed the issue of safe screw drilling distance. However, in the present study, both distances referring to the superior and posterior screws were smaller than those previously published, especially when compared with the Caucasian population.

According to the clock face indication system, the modified danger zone was oriented between the two o'clock and eight o'clock positions in reference to the right shoulder. As illustrated in Fig. 4, the projections of points B and C were defined as danger zone I, regarding the short safe distance and the adjacent position with origin of coordinates. The suprascapular nerve is more vulnerable to injury by the posterior fixation screw in danger zone I. While in danger zone II, defined by

the projection area of point A, a relatively longer safe distance for superior fixation screw is permitted. Similarly, a cadaveric study by Molony et al. [8] concluded that the baseplate fixation during RSA, the posterior screw exhibited a more significant risk than the superior screw, which carries the risk of injuring both the main trunk and glenohumeral articular branch of the suprascapular nerve. A safe border of the glenoid rim has been recommended by Nathan et al. to be the vertical axis across the supraglenoid and infraglenoid tubercle [10]. Our findings also confirmed that the suprascapular nerve is potentially at risk by the superior screw anterior to the safe border.

We also noticed a significant difference in safe distances between male and female patients. In addition, the limiting screw
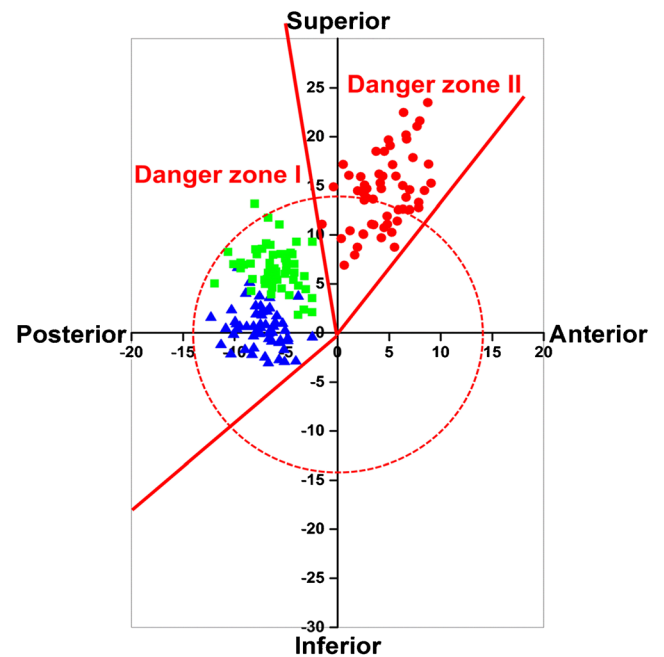
Table 3 Pearson correlation coefficient analysis between the morphological size of the glenoid fossa and the distances referring to the safe zone

Glenoid fossa parameter	a (p value)	b (p value)	c (p value)
h	0.41 (0.00)	0.36 (0.01)	0.44 (0.00)
w	0.54 (0.00)	0.36 (0.01)	0.48 (0.00)
r	0.53 (0.00)	0.38 (0.00)	0.49 (0.00)

Abbreviations: h, height of the glenoid fossa; w, width of the glenoid fossa; r, radius of the best-fit circle (baseplate); a, b, and c, safe distances of projections to the cutting plate from A, B and C, respectively; A, suprascapular notch; B and C, bony border of the base of the scapular spine

Fig. 4 The projections of the bony reference points to the cutting plane in the reference of the right shoulder. *Red dots* represent projections of point A, *green diamonds* represent projections of point B, and *blue triangles* represent projections of point C. **a** Suprascapular notch. **b** and **c** Bony border of the base of the scapular spine. The *red dashed circle* represents the standard baseplate

Table 4 Measurements of suprascapular notch and spinoglenoid notch in previously published literature compared with the present study

Literature	Suprascapular notch (cm)		Spinoglenoid notch (cm)	
	Average	Range	Average	Range
Bigliani et al. [35] (United States 1990)	3.0	2.5–3.9	1.8	1.4–2.5
Ekin et al. [36] (Unites States 1995)	3.3	2.1–3.8	2.0	1.3–2.4
Shishido et al. [15] (Japan 2001)	2.9	2.3–3.5	1.8	1.4–2.4
Gumina et al. [13] (Italy 2010)	3.1	2.1–4.1	1.7	1.1–2.5
Hawi et al. [37] (Germany 2015)	3.3	3.1–3.5	2.1	2.0–2.2
Pérez et al. [38] (Spain 2016)	3.5	3–4.1	2.4	1.9–3.1
Mathews [31] (Switzerland 2017)	3.3	2.6–3.9	–	–
Current study (China 2017)	3.0	2.5–3.8	1.7	1.3–2.0

distances were found to be positively related to the glenoid size. Our data suggested that a personalized 3D model based on a CT scan is essential, not only to estimate glenoid size and bone stock of the scapula, but also to perform accurate preoperative planning for RSA. Careful considerations of the length and orientation of the screws must be taken to minimize the risk of nerve injury.

One of the limitations of this study is the small sample size. Secondly, all the measurements in the present study were based on the selected bony references instead of exact structures in previous cadaveric studies. However, the course of the nerve is relatively fixed in the corresponding bony notches as reported [8]. Furthermore, the results of statistical analysis indicated reliable reproducibility. Finally, only patients with PHF were included in this study to evaluate the morphological features of a normal glenoid cavity. Considering there are a variety of deformed changes in arthritic glenoid cavities due to the severity of erosion [39], subsequent investigations will be performed to evaluate the morphological features in various arthritic groups.

Using 3D reconstruction and simulated segmentation, we provided a morphological analysis of glenoid size in the Chinese population. As indicated in the literature, standard components are not adequate for RSA implantation in the Chinese population, especially in small female patients. Furthermore, a novel method based on simulated projection was presented in this study to define a safe zone of the glenoid fossa. During baseplate fixation in RSA, the distance of the posterior and superior screws should be carefully considered to avoid injury of the suprascapular nerve.

Compliance with ethical standards

Conflict of interest On behalf of all authors, the corresponding author states that there is no conflict of interest.

References

1. Bachman D, Nyland J, Krupp R (2016) Reverse-total shoulder arthroplasty cost-effectiveness: a quality-adjusted life years comparison with total hip arthroplasty. World J Orthop 7(2):123–127. https://doi.org/10.5312/wjo.v7.i2.123

2. Dezfuli B, King JJ, Farmer KW, Struk AM, Wright TW (2016) Outcomes of reverse total shoulder arthroplasty as primary versus revision procedure for proximal humerus fractures. J Shoulder Elbow Surg 25(7):1133–1137 https://doi.org/10.1016/j.jse.2015.12.002

3. Ji JH, Shafi M, Jeong JJ, Ha JY (2016) Reverse total shoulder arthroplasty in the treatment of chronic anterior fracture dislocation complicated by a chronic full thickness retracted rotator cuff tear in an elderly patient. J Orthop Science 21(2):237–240. https://doi.org/10.1016/j.jos.2015.06.004

4. Longo UG, Forriol F, Loppini M, Lanotte A, Salvatore G, Maffulli N, Denaro V (2015) The safe zone for avoiding suprascapular nerve injury in bone block procedures for shoulder instability. A cadaveric study. Knee Surg Sports Traumatol Arthrosc 23(5):1506–1510. https://doi.org/10.1007/s00167-014-2900-1

5. Avery BW, Pilon FM, Barclay JK (2002) Anterior coracoscapular ligament and suprascapular nerve entrapment. Clin Anatomy (New York, NY) 15(6):383–386. https://doi.org/10.1002/ca.10058

6. Dwyer T, Henry PD, Cholvisudhi P, Chan VW, Theodoropoulos JS, Brull R (2015) Neurological complications related to elective orthopedic surgery: part 1: common shoulder and elbow procedures. Reg Anesth Pain Med 40(5):431–442. https://doi.org/10.1097/aap.0000000000000178

7. Kempton LB, Ankerson E, Wiater JM (2011) A complication-based learning curve from 200 reverse shoulder arthroplasties. Clin Orthop Relat Res 469(9):2496–2504. https://doi.org/10.1007/s11999-011-1811-4

8. Molony DC, Cassar Gheiti AJ, Kennedy J, Green C, Schepens A, Mullett HJ (2011) A cadaveric model for suprascapular nerve injury during glenoid component screw insertion in reverse-geometry shoulder arthroplasty. J Shoulder Elbow Surg 20(8):1323–1327. https://doi.org/10.1016/j.jse.2011.02.014

9. Wang J, Singh A, Higgins L, Warner J (2010) Suprascapular neuropathy secondary to reverse shoulder arthroplasty: a case report. J Shoulder Elbow Surg 19(3):e5–e8. https://doi.org/10.1016/j.jse.2009.10.004

10. Hart ND, Clark JC, Wade Krause FR, Kissenberth MJ, Bragg WE, Hawkins RJ (2013) Glenoid screw position in the encore reverse shoulder prosthesis: an anatomic dissection study of screw relationship to surrounding structures. J Shoulder Elbow Surg 22(6):814–820. https://doi.org/10.1016/j.jse.2012.08.013

11. Shi LL, Freehill MT, Yannopoulos P, Warner JJ (2012) Suprascapular nerve: is it important in cuff pathology? Adv Orthop 2012:516985. https://doi.org/10.1155/2012/516985

12. Levigne C, Boileau P, Favard L, Garaud P, Mole D, Sirveaux F, Walch G (2008) Scapular notching in reverse shoulder arthroplasty. J Shoulder Elbow Surg 17(6):925–935. https://doi.org/10.1016/j.jse.2008.02.010

13. Gumina S, Albino P, Giaracuni M, Vestri A, Ripani M, Postacchini F (2011) The safe zone for avoiding suprascapular nerve injury during shoulder arthroscopy: an anatomical study on 500 dry scapulae. J Shoulder Elbow Surg 20(8):1317–1322. https://doi.org/10.1016/j.jse.2011.01.033

14. Middernacht B, De Roo PJ, Van Maele G, De Wilde LF (2008) Consequences of scapular anatomy for reversed total shoulder arthroplasty. Clin Orthop Relat Res 466(6):1410–1418. https://doi.org/10.1007/s11999-008-0187-6

15. Shishido H, Kikuchi S (2001) Injury of the suprascapular nerve in shoulder surgery: an anatomic study. J Shoulder Elbow Surg 10(4):372–376. https://doi.org/10.1067/mse.2001.115988

16. Levy JC, Everding NG, Frankle MA, Keppler LJ (2014) Accuracy of patient-specific guided glenoid baseplate positioning for reverse shoulder arthroplasty. J Shoulder Elbow Surg 23(10):1563–1567

17. Dilisio MF, Warner JJ, Walch G (2016) Accuracy of the Subchondral smile and surface referencing techniques in reverse shoulder Arthroplasty. Orthopedics 39(4):e615–e620

18. Trouilloud P, Gonzalvez M, Martz P, Charles H, Handelberg F, Nyffeler R, Baulot E (2014) Duocentric® reversed shoulder prosthesis and personal fit® templates: innovative strategies to optimize prosthesis positioning and prevent scapular notching. Eur J Orthop Surg Traumatol 24(4):483–495

19. Lewis GS, Bryce CD, Davison AC, Hollenbeak CS, Piazza SJ, Armstrong AD (2010) Location of the optimized centerline of the glenoid vault: a comparison of two operative techniques with use of three-dimensional computer modeling. J Bone Joint Surg Am 92(5):1188–1194. https://doi.org/10.2106/jbjs.i.00131

20. Denard PJ, Lederman E, Parsons BO, Romeo AA (2016) Finite element analysis of glenoid-sided lateralization in reverse shoulder arthroplasty. J Orthopaedic Res 35(7):1548–1555. https://doi.org/10.1002/jor.23394

21. Ji JH, Jeong JY, Song HS, Ok JH, Yang SJ, Jeon BK, Kim TG, Moon YS, Kim YS (2013) Early clinical results of reverse total shoulder arthroplasty in the Korean population. J Shoulder Elbow Surg 22(8):1102–1107. https://doi.org/10.1016/j.jse.2012.07.019

22. Stephens BF, Hebert CT, Azar FM, Mihalko WM, Throckmorton TW (2015) Optimal baseplate rotational alignment for locking-screw fixation in reverse total shoulder arthroplasty: a three-dimensional computer-aided design study. J Shoulder Elbow Surg 24(9):1367–1371. https://doi.org/10.1016/j.jse.2015.01.012

23. Faul F, Erdfelder E, Lang A-G, Buchner A (2007) G* power 3: a flexible statistical power analysis program for the social, behavioral, and biomedical sciences. Behav Res Methods 39(2):175–191

24. Xiao J, Wang C, Zhu L, Li X, Liu T, Wang Q, Qin Y (2014) Improved method for planning intramedullary guiding rod entry point in total knee arthroplasty. Arch Orthop Trauma Surg 134(5):693–698. https://doi.org/10.1007/s00402-014-1943-6

25. Ricchetti ET, Hendel MD, Collins DN, Iannotti JP (2013) Is premorbid glenoid anatomy altered in patients with glenohumeral osteoarthritis? Clin Orthop Relat Res 471(9):2932–2939. https://doi.org/10.1007/s11999-013-3069-5

26. Nam D, Kepler CK, Nho SJ, Craig EV, Warren RF, Wright TM (2010) Observations on retrieved humeral polyethylene components from reverse total shoulder arthroplasty. J Shoulder Elbow Sur 19(7):1003–1012. https://doi.org/10.1016/j.jse.2010.05.014

27. Jha SC, Fukuta S, Wada K, Higasino K, Amari-Kita R, Tsutsui T, Goto T, Hamada D, Suzue N, Matsuura T, Nishisho T, Abe M, Takata Y, Sakai T, Nagamachi A, Sairyo K (2016) Optimizing baseplate position in reverse total shoulder arthroplasty in small-sized Japanese females: technical notes and literature review. J Medical Investig 63(1-2):8–14. https://doi.org/10.2152/jmi.63.8

28. DiStefano JG, Park AY, Nguyen TQ, Diederichs G, Buckley JM, Montgomery WH 3rd (2011) Optimal screw placement for base plate fixation in reverse total shoulder arthroplasty. J Shoulder Elbow Surg 20(3):467–476. https://doi.org/10.1016/j.jse.2010.06.001

29. Moineau G, Levigne C, Boileau P, Young A, Walch G (2012) Three-dimensional measurement method of arthritic glenoid cavity morphology: feasibility and reproducibility. Orthop Traumatol Surg Res 98(6 Suppl):S139–S145. https://doi.org/10.1016/j.otsr.2012.06.007

30. Matsumura N, Oki S, Ogawa K, Iwamoto T, Ochi K, Sato K, Nagura T (2016) Three-dimensional anthropometric analysis of the glenohumeral joint in a normal Japanese population. J Shoulder Elbow Surg 25(3):493–501. https://doi.org/10.1016/j.jse.2015.08.003

31. Mathews S, Burkhard M, Serrano N, Link K, Hausler M, Frater N, Franke I, Bischofberger H, Buck FM, Gascho D, Thali M, Serowy S, Muller-Gerbl M, Harper G, Qureshi F, Boni T, Bloch HR, Ullrich O, Ruhli FJ, Eppler E (2017) Glenoid morphology in light of anatomical and reverse total shoulder arthroplasty: a dissection- and 3D-CT-based study in male and female body donors. BMC Musculoskelet Disord 18(1):9. https://doi.org/10.1186/s12891-016-1373-4

32. Piponov HI, Savin D, Shah N, Esposito D, Schwartz B, Moretti V, Goldberg B (2016) Glenoid version and size: does gender, ethnicity, or body size play a role? Int Orthop 40(11):2347–2353. https://doi.org/10.1007/s00264-016-3201-8

33. Chae SW, Kim SY, Lee H, Yon JR, Lee J, Han SH (2014) Effect of baseplate size on primary glenoid stability and impingement-free range of motion in reverse shoulder arthroplasty. BMC Musculoskelet Disord 15:417. https://doi.org/10.1186/1471-2474-15-417

34. Churchill RS, Brems JJ, Kotschi H (2001) Glenoid size, inclination, and version: an anatomic study. J Shoulder Elbow Surg 10(4):327–332. https://doi.org/10.1067/mse.2001.115269

35. Bigliani LU, Dalsey RM, McCann PD, April EW (1990) An anatomical study of the suprascapular nerve. Arthroscopy 6(4):301–305

36. Ekin A, Magden O, Iche C (1995) Anatomy and relationship of the suprascapular nerve. Surgery of the shoulder. Elsevier, NY

37. Hawi N, Reinhold A, Suero EM, Liodakis E, Przyklenk S, Brandes J, Schmiedl A, Krettek C, Meller R (2016) The anatomic basis for the arthroscopic Latarjet procedure: a cadaveric study. Am J Sports Med 44(2):497–503. https://doi.org/10.1177/0363546515614320

38. Perez A, Navas I, Herencias A, Marco F, Sanudo J, Simon C, Vazquez T (2016) Morphometry of the suprascapular nerve in the supraspinous fossa. Eur J Anat 20(3):215–220

39. Frankle MA, Teramoto A, Luo Z-P, Levy JC, Pupello D (2009) Glenoid morphology in reverse shoulder arthroplasty: classification and surgical implications. J Shoulder Elb Surg 18(6):874–885